Hadley Centre Technical Note 87

Mineral Dust in HadGEM2

March 2011

Stephanie Woodward

Mineral Dust in HadGEM2

Stephanie Woodward
Met Office Hadley Centre, Fitzroy Road, Exeter, EX1 3PB, United Kingdom

Introduction

The radiative effect of aerosols is an important aspect of the climate system, and radiative forcing by mineral dust is a significant contributor to this. In addition, mineral dust affects climate through ecosystem interactions such as the provision of iron which in certain areas impacts phytoplankton growth and thus DMS emissions and sulphate aerosols as well as the ocean carbon cycle. The creation of the first earth systems models which include not only the physical atmosphere and ocean but also global biogeochemical processes means that it is more important than ever for models to have a realistic simulation of mineral dust aerosol. The HadGEM2-ES model is among the first of this new generation of earth systems models (Collins et al, 2011).
The dust scheme used in HadGEM2-ES and the parallel coupled and atmospheric GCMs HadGEM2-AO and HadGEM2-A is based on that originally created for the HadAM3 (Woodward, 2001), but with significant improvements to the emissions model and updated spectral radiative properties. This technical note presents these developments and their impact on dust simulations in the HadGEM2 model family.

The HadGEM2 Models

Development of the dust scheme was performed within the framework of the HadGEM2 model (Collins et al. 2011, The HadGEM2 Development Team, 2011). Three model configurations were used for dust experiments: (1) HadGEM2-A, atmospheric GCM, run with prescribed SSTs ; (2) HadGEM2-AO, coupled atmosphere ocean climate model, freely running with inputs such as trace gas and aerosol emissions set appropriately for the period of the simulation; (3) HadGEM2-ES, the full earth system model, including biogeochemical interactions such as an interactive vegetation scheme, ocean biogeochemistry etc., with emissions appropriate to the period. Experiments described here were run at N96 resolution with 38 vertical levels.

Dust Emission Scheme

Dust emissions are calculated each 30-minute timestep using the prognostic model fields. The dust emission scheme utilises the widely-used algorithm of Marticorena and Bergametti (1995) to calculate horizontal flux in each of 9 bins with boundaries at 0.0316, 0.1, 0.316, 1., 3.16, 10., 31.6, 100., 316.and 1000. micron radius:

$$G_i = \rho\,(1-V)\,U^{*3}\,(1+U^*_{ti}/U^*)\;(1-(U^*_{ti}/U^*)^2)\;M_i\;C\;S\,/\,g \qquad (1)$$

where i refers to bin number, G is horizontal flux, ρ is air density at the surface, V is vegetation fraction in the grid-box, U^*_t is threshold friction velocity, U* is friction

velocity, M is mass fraction of soil particles in the bin, C is a constant of proportionality, set to 2.61 from wind-tunnel experiments, S is a preferential source term and g is acceleration due to gravity. This equation was derived from experimental measurements, essentially at point sources at a single time, whereas the model calculates grid-box mean, time-step mean values.
In order to correct for the effect of this spatial and temporal averaging, U* in equation (1) is calculated from the model value U^*_M and a tuneable constant k_1:

$$U^* = k_1 U^*_M \quad (2)$$

k_1 is obtained empirically, by performing simulations with a range of values to minimise errors in dust concentrations and optical depth compared with observations. Inevitably, the value chosen will be influenced by biases in model fields as well as by the resolution of the model.
Vegetation fraction is taken from the model. HadGEM2-A and HadGEM2-AO use IGBP data. In HadGEM2-ES vegetation fraction is calculated interactively by the TRIFFID dynamic vegetation scheme (Cox, 2001).
The mass fraction of particles in each bin (M) is calculated off-line from the clay/silt/sand fraction data from IGBP, for consistency with other soil properties used in the model. The method used is based on that described in Woodward (2001), extended to cover the full particle size range used here.
Emissions are inhibited if the surface is snow-covered or frozen, and on steep slopes and coastal points, where wind-speeds may be anomalously high.
Dry threshold friction velocity (U^*_{td}) for each bin is taken from Bagnold (1941). The effect of soil moisture is treated according to the method of Fécan et al. (1999), which has been shown to be in good agreement with observations. This relates threshold friction velocity in moist and dry conditions by:

$$U^*_t/U^*_{td} = 1 \text{ for } w<w'$$

$$U^*_t/U^*_{td} = (1 + 1.21(w-w')^{0.68})^{0.5} \text{ for } w>w' \quad (3)$$

$$w' = 0.14 * F_C^2 + 17.0 * F_C$$

where F_C is clay fraction and w represents volumetric soil moisture. In order to relate this point value to the model's grid-box mean soil moisture over the top 10cm soil level (w_1), a tuneable constant is applied, in a similar manner to that for friction velocity:

$$w = k_2 * w_1 \quad (4)$$

In order to apply the Fécan et al. scheme to moister regions than the arid and semi-arid areas for which it was designed, a further restriction is put on dust emissions from moist soils. Emissions are inhibited when soil moisture exceeds a threshold, depending on particle size.

$$w_t = (F_C + 0.12)/ 0.03 \quad (5)$$

This limit corresponds approximately to the maximum soil moisture at which soil movement was observed in the measurements used by Fécan et al.

Vertical dust flux is calculated for 6 bins corresponding to those of the horizontal flux up to 31.6 μm radius. The size distribution follows that of the horizontal flux in these bins, but total vertical flux is related to total horizontal flux across all 9 bins following the formulation of Marticorena and Bergametti (1995) based on the measurements of Gillette (1979). Thus the vertical flux in bin i (F_i), for i=1 to 6 is given by:

$$F_i = 10^{(13.4\,Fc - 6.0)} \quad G_i \quad \Sigma_{i=1,9}(G_i) / \Sigma_{i=1,6}(G_i) \qquad (6)$$

A maximum of 0.2 was applied to F_C (clay fraction), as this was the highest clay fraction in the observations on which the algorithm was based and higher values of F_C resulted in unrealistically high dust emissions.

Preferential sources have become widely used in dust emission schemes in recent years (e.g. Ginoux et al, 2001; Tegen et al, 2002). A preferential source term represents the probability of the presence of accumulated erodible sediment in a grid-box by relating this to a more readily available variable such as topography, the locations of paleo-lakes or runoff areas. These variants all produce broadly similar results (Zender and Newman, 2003). We have chosen to use a multiplier based on the formulation of Ginoux et al (2001):

$$S = \left((z_{max} - z_i) / (z_{max} - z_{min}) \right)^{P}$$

where S represents the probability of the presence of accumulated sediment, z_{max}, z_{min} and z_i are maximum, minimum and local altitude in an area approximately $10^o x 10^o$ and P is an empirically chosen term, set to 3 here to give the best simulation of dust concentrations and AODs compared with observations. Altitudes were calculated at N320 – the highest readily available resolution in the global Unified Model - and then re-gridded to the N96 model resolution. Figure 1 shows the global distribution of the preferential source term.

Dust Transport and Deposition

The transport and deposition of dust is as described in detail in Woodward (2001). The dust is treated as 6 independent tracers in the atmosphere, corresponding to the 6 bins of the vertical dust flux. Dry deposition through sedimentation and turbulent mixing, as well as wet deposition processes are modelled.

Radiative Properties

Dust interacts with the GCM through shortwave and longwave direct effects. Extinction coefficients, single scattering albedos and asymmetry parameters were calculated from refractive indices, using Mie theory, assuming spherical particles. The refractive index data of Balkanski et al (2007) for Saharan dust was used.

Dust Simulations

Results from a 22-year HadGEM2-A simulation are presented below. In this experiment the SSTs for 1978-2000 were prescribed, but the model was otherwise free-running. Figure 2 shows 20 year mean emissions and atmospheric load and figure 3 shows a comparison of modelled near-surface concentrations and AODs with observations from stations of the University of Miami network (provided by J. Prospero and D. Savoie) and AERONET stations. Stations were chosen for which a minimum of 4 years data was available, and the AERONET stations were in locations where mineral dust was the dominant aerosol. The distribution of dust emissions and load appears to be reasonably realistic and the agreement with observations is generally good. AODs are well-simulated at locations where dust dominates. Concentrations in the Atlantic are well-simulated across the whole length of the Saharan plume. In the Pacific concentrations at some stations are a little high, particularly in spring, due to anomalous emissions from regions around the Arabian Sea, except at Cheju, where concentrations are low due to insufficient emissions from Chinese deserts. Concentrations in the Southern Ocean are mostly in good agreement with observations, though short-lived peaks in observations from the Antarctic Peninsula in the Austral autumn and winter (not shown) are not replicated by the model.

The development of HadGEM2-AO and HadGEM2-ES was undertaken in the usual way, for the pre-industrial period in order to allow the models to reach equilibrium under pre-industrial conditions before transient experiments up to and beyond the present day were performed. As very few historical observations of dust are available, the dust scheme in these models was, of necessity, tuned to present-day values in a historical climate. Though this method inevitably leads to sub-optimal present-day dust simulations, the errors introduced are not large in relation to others caused by general model biases. Mineral dust emissions are very highly sensitive to model fields, particularly wind-speed, but also soil moisture and soil particle size distribution, which are all poorly constrained in the remote arid areas where most dust production occurs. As a result of this, quite modest biases in these fields can lead to significant biases in dust concentrations and it is to be expected that the impact of the model climate on dust simulations should dominate over the effect of anachronistic tuning. Figure 4 shows decadal mean simulated dust loads for the pre-industrial period for HadGEM2-AO and HadGEM2-ES, and for the decade 1990-2000 from a transient HadGEM2-ES experiment, and comparisons with observations. It can be seen that results are broadly similar to those from HadGEM2-A. Results from HadGEM2-AO show better agreement with observations than those from HadGEM2-ES, as might be expected from a more closely constrained model.

Conclusions

Significant developments have been made to the Hadley Centre dust scheme for its implementation with the HadGEM2 suite of models. Results have been shown to be in generally good agreement with observations in each of the HadGEM2-A, HadGEM2-AO and HadGEM2-ES models, and the scheme provides a good capability for studying the interactions between dust and climate within the framework of these GCMs.

References

Balkanski, Y. et al., Reevaluation of Mineral aerosol radiative forcings suggests a better agreement with satellite and AERONET data, Atmos. Chem. Phys. 7, 2007.

Collins W. et al., Development and evaluation of an earth-system model – HadGEM2, Geophysical Model Development, 2011 (in prep.)

Cox, P. M., Description of the TRIFFID Dynamic Global vegetation Model, Met Office Hadley Centre Technical Note 24, 2001.

Fécan, F. et al, Parametrization of the increase of the Aeolian erosion threshold wind friction velocity due to soil moisture for arid and semi-arid areas, Ann. Geophys. 17, 1999

Gillette, D.A., Environmental factors affecting dust emissions by wind erosion., *Saharan Dust*, ed. C Morales, John Wiley, New York, 1979.

Ginoux, P. et al, Sources and distributions of dust aerosols simulated with the GOCART model., J. Geophys. Res. 106, D17, 2001.

Marticorena, B. and Bergametti, G., Modelling the atmospheric dust cycle: 1. Design of a soil-derived dust emission scheme., J. Geophys. Res. 100, D8, 1995.

Martin, G et al., The HadGEM2 family of Met Office Unified Model Climate Configurations, 2011 (in preparation).

Tegen, I. et al, Impact of vegetation and preferential source areas on global dust aerosol: Results from a model study., J. Geophys. Res. 107, D21, 2002.

Woodward, S., Modeling the atmospheric life cycle and radiative impact of mineral dust in the Hadley Centre climate model., J. Geophys. Res., 106, D16, 2001.

Zender, C. S. and Newman, D., Spatial heterogeneity in Aeolian erodibility: Uniform, topographic, geomorphic, and hydrologic hypotheses., J. Geophys. Res., 108, D17, 2003.

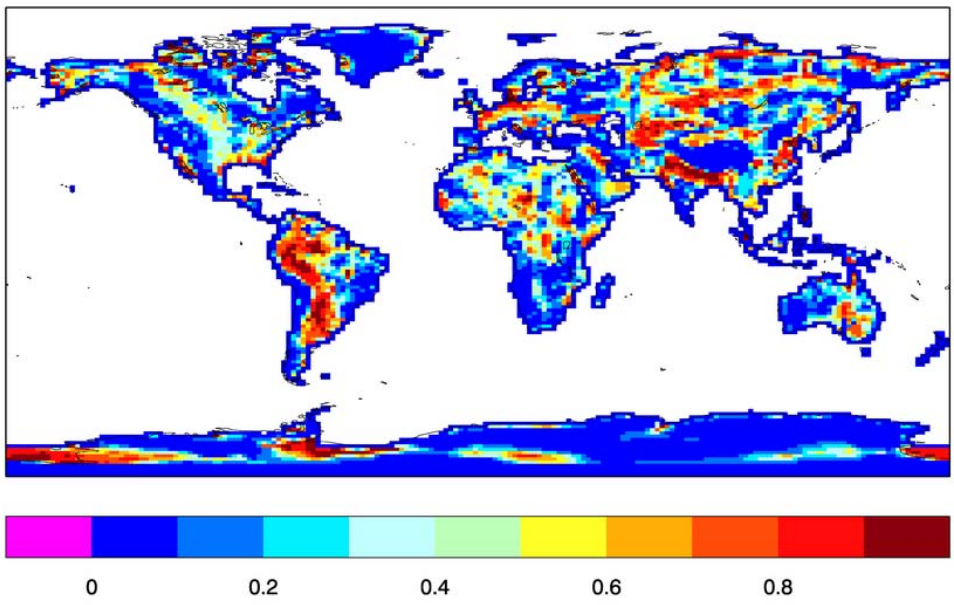

Figure 1. Preferential source multiplier.

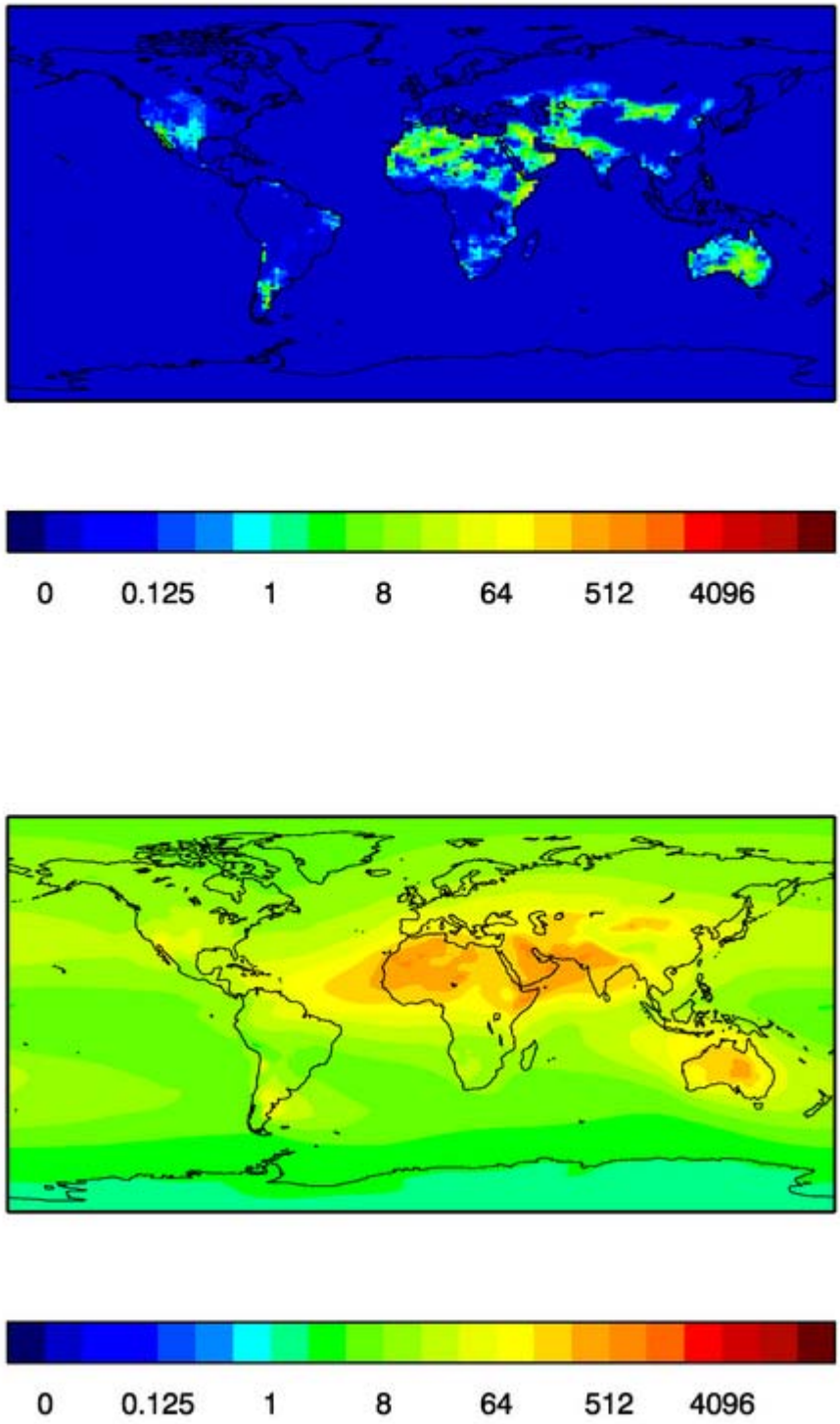

Figure 2. Twenty year mean dust emissions (μg m^{-2} s^{-1}) (above) and load (mg m^{-2}) (below) from a HadGEM2-A simulation.

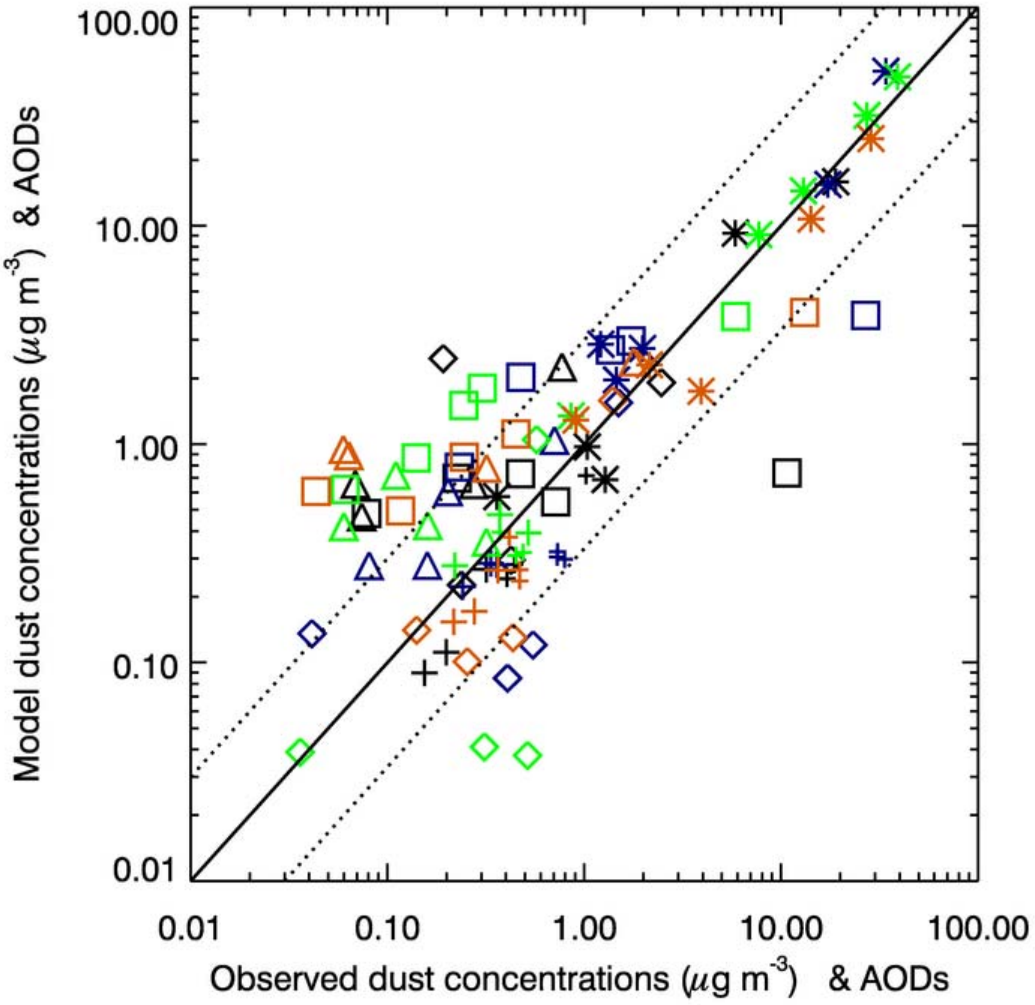

Figure 3. Seasonal mean near-surface concentrations and AODs from a 22-year HadGEM2-A experiment compared with observations from the University of Miami network and AERONET stations respectively. Colours represent seasons: black – DJF, blue – MAM, green – JJA, red – SON. Symbols represent observational stations: large plus – AERONET stations where dust dominates (Cap Verde, Solar Village, SedeBoker), small plus - AERONET stations where both dust and biomass burning are important (Banizoubou, Ouagadougou, Ilorin); asterisk – Atlantic stations (Izana, Miami, Mace Head, Bermuda, Barbados); square – N Pacific stations (Enewetak, Fanning, Cheju, Oahu, Midway); triangle – S Pacific stations (American Samoa, Norfolk Island, Nauru, Funafuti); diamond – Southern Ocean stations (Cape Grim, King George Island, Mawson, Palmer).

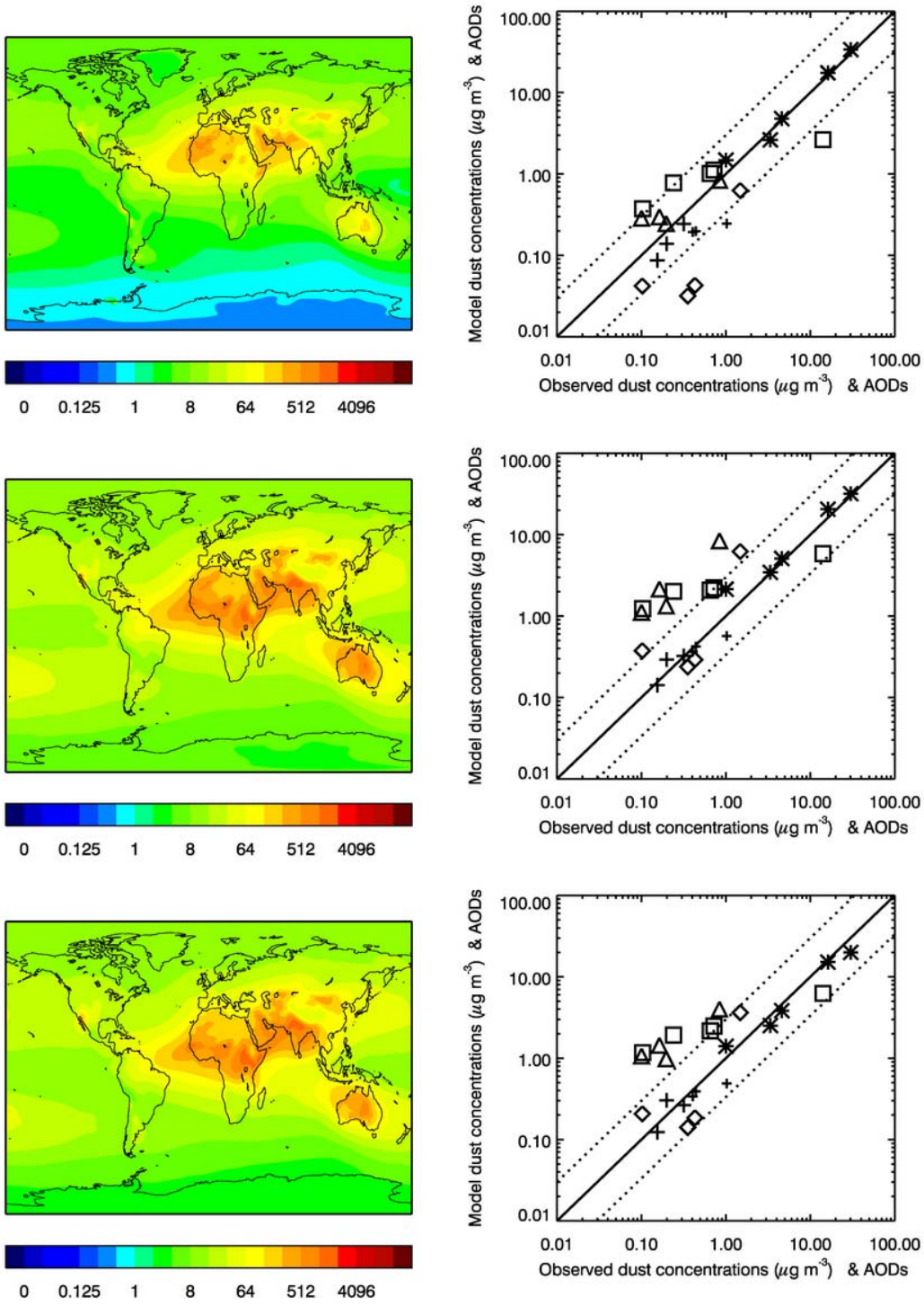

Figure 4. Decadal mean dust load (mg m^{-2}) and comparison of near-surface concentrations and AODs with observations from HadGEM2-AO pre-industrial simulation (top), HadGEM2-ES pre-industrial simulation (middle) and HadGEM2-ES present-day simulation (bottom). Symbols as in figure 3.

Met Office
FitzRoy Road, Exeter
Devon, EX1 3PB
UK

Tel: 0870 900 0100
Fax: 0870 900 5050
enquiries@metoffice.gov.uk
www.metoffice.gov.uk